Proc. Natl. Acad. Sci. USA
Vol. 88, pp. 7328–7332, August 1991
Cell Biology

Modeling the cell division cycle: cdc2 and cyclin interactions

(maturation promoting factor/metaphase arrest/*wee1*/*cdc25*)

JOHN J. TYSON

Department of Biology, Virginia Polytechnic Institute and State University, Blacksburg, VA 24061

Communicated by David M. Prescott, May 20, 1991 (received for review January 23, 1991)

ABSTRACT **The proteins cdc2 and cyclin form a heterodimer (maturation promoting factor) that controls the major events of the cell cycle. A mathematical model for the interactions of cdc2 and cyclin is constructed. Simulation and analysis of the model show that the control system can operate in three modes: as a steady state with high maturation promoting factor activity, as a spontaneous oscillator, or as an excitable switch. We associate the steady state with metaphase arrest in unfertilized eggs, the spontaneous oscillations with rapid division cycles in early embryos, and the excitable switch with growth-controlled division cycles typical of nonembryonic cells.**

Passage through the cell cycle is marked by a temporally organized sequence of events including DNA replication, mitosis, and the appearance of certain cell-cycle specific proteins and enzymatic activities (1). In most populations of proliferating cells, the processes of growth and division occur simultaneously and are coordinated by some mechanism that monitors the nucleocytoplasmic ratio of a cell and triggers cell division at a characteristic value of this ratio (2–4). In contrast, during oogenesis the developing egg accumulates great quantities of maternal cytoplasm while undergoing a reductive nuclear division, so the nucleocytoplasmic ratio becomes abnormally small. After fertilization the developing embryo undergoes many cycles of DNA synthesis and nuclear division in the absence of cell growth, to bring the nucleocytoplasmic ratio back to values typical of somatic cells. The division cycles of an early embryo are extremely rapid (30 min in frog embryos) until the midblastula transition (MBT) (5, 6). Furthermore, if the nucleus is removed from a fertilized frog egg, the enucleated cell continues to undergo periodic cortical contractions at 30-min intervals, as if it were trying to divide (7). Enucleated sea urchin eggs even undergo cleavage and develop into abnormal blastulas (8). As Mazia (9) puts it, the cell cycle is really a cell "bicycle;" the two wheels are the growth cycle and the division cycle, which normally turn in a 1:1 ratio but may turn independently.

The mitotic cycles in both embryonic and somatic cells appear to be controlled by the activity of an enzyme, maturation promoting factor (MPF), that peaks abruptly at metaphase (10–14). MPF is a heterodimer composed of cyclin (M_r = 45,000) and a protein kinase (M_r = 34,000) (15, 16). The protein kinase is sometimes called p34, in reference to its apparent molecular weight, and sometimes called cdc2, in reference to the gene (*cdc2*) that codes for the protein in fission yeast.

The interplay between cyclin and cdc2 in generating MPF activity is understood in some detail (see Fig. 1) (10–14). Newly synthesized cyclin subunits combine with preexisting cdc2 subunits to form an inactive MPF complex. The complex is then activated, in an autocatalytic fashion (17), by dephosphorylation at a specific tyrosine residue of the cdc2 subunit (18). Active MPF is known to stimulate a number of processes essential for nuclear and cell division (13, 14). At the transition from metaphase to anaphase, the MPF complex dissociates, and the cyclin subunit is rapidly degraded (15, 19–21). Then the cycle repeats itself.

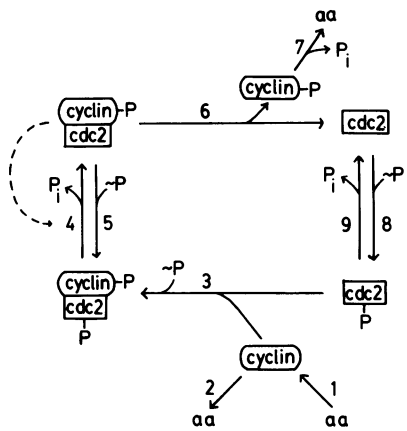

FIG. 1. The relationship between cyclin and cdc2 in the cell cycle. In step 1, cyclin is synthesized *de novo*. Newly synthesized cyclin may be unstable (step 2). Cyclin combines with cdc2-*P* (step 3) to form "preMPF." At some point after heterodimer formation, the cyclin subunit is phosphorylated. (Assuming phosphorylation is faster than dimerization, I write the two-step process as a single step, rate-limited by dimerization.) The cdc2 subunit is then dephosphorylated (step 4) to form "active MPF." In principle, the activation of MPF may be opposed by a protein kinase (step 5). Assuming that active MPF enhances the catalytic activity of the phosphatase (as indicated by the dashed arrow), I arrange that MPF activation is switched on in an autocatalytic fashion. Nuclear division is triggered when a sufficient quantity of MPF has been activated, but concurrently active MPF is destroyed by step 6. Breakdown of the MPF complex releases phosphorylated cyclin, which is subject to rapid proteolysis (step 7). Finally, the cdc2 subunit is phosphorylated (step 8, possibly reversed by step 9), and the cycle repeats itself. aa, amino acids; ~P, ATP; P_i, inorganic phosphate.

MPF dissociation and cyclin proteolysis are necessary to complete the mitotic cycle: metaphase arrest of unfertilized eggs corresponds to steady high levels of active MPF, and fertilization releases the egg from metaphase by stimulating the breakdown of the active MPF complex (10). In early embryos, the cycle of MPF activation and deactivation seems to be controlled by the synthesis of cyclin (21, 22), although some evidence suggests that posttranslational events may be rate-limiting (12, 23). In any event, the cycle continues even in the absence of DNA synthesis (24). In somatic cells, by contrast, cyclin synthesis is not sufficient to activate MPF, and the MPF cycle is dependent on cell growth and periodic DNA synthesis (12). In fission yeast, activation of the MPF complex is controlled by at least two other gene products: wee1, an inhibitor of MPF, and cdc25, an activator (25, 26). These two proteins apparently monitor the nucleocytoplasmic ratio in the yeast cell and activate MPF at a critical value

The publication costs of this article were defrayed in part by page charge payment. This article must therefore be hereby marked "*advertisement*" in accordance with 18 U.S.C. §1734 solely to indicate this fact.

Abbreviations: MPF, maturation promoting factor (also called M-phase-promoting factor); MBT, midblastula transition.

of this ratio, although it is not clear at present just how the (size) control works.

The model summarized in Fig. 1 is adapted from many sources (12, 14, 16, 27–29), but it is still a highly simplified view of cdc2–cyclin interactions. It concentrates on dephosphorylation of tyrosine-15 but ignores the activating phosphorylation of threonine-167 (14, 30, 47). It attributes cyclin degradation to phosphate labeling instead of conjugation with ubiquitin (48), and it ignores the apparent stimulatory effect of active MPF on cyclin degradation (29).

Despite such simplifications and omissions, the model in Fig. 1 is a reasonable "first approximation" to the cell-cycle regulatory network. How good is this picture? Can it account for the coordination of cell growth and division during the normal (somatic) cell cycle? How is the nucleocytoplasmic ratio measured and how is this information communicated to the cyclin–cdc2 mitotic-triggering complex? Can the same model also account for metaphase arrest of unfertilized eggs, for rapid cycles of DNA synthesis and cell division (without cell growth) during the embryonic cell cycle, and for the autonomous cycling of MPF activity in the absence of DNA synthesis or cell division in enucleated embryos?

To answer these questions I frame the model in Fig. 1 in precise mathematical equations (Table 1) and investigate the properties of these equations. This approach makes evident the precise consequences of the assumptions about cdc2–cyclin interactions implicit in Fig. 1. To the extent that these consequences are in accord with observations, we gain confidence in our understanding of cell-cycle regulation. Where the consequences are out of accord, we have a framework in which to analyze and compare alternative assumptions about the control system.

Steady States and Oscillations

Solutions of the equations in Table 1 depend on the values assumed by the 10 parameters in the model (Table 2). Nothing is known experimentally about appropriate values for these parameters, so I can demonstrate at present only that there exist numerical values of the parameters for which the model exhibits dynamical behavior reminiscent of cell-cycle control.

In this report I focus on two parameters: k_4, the rate constant describing the autocatalytic activation of MPF by dephosphorylation of the cdc2 subunit, and k_6, the rate constant describing breakdown of the active cdc2–cyclin complex. Depending on the values of k_4 and k_6 (Fig. 2), there are regions of stable steady-state behavior (regions A and C) and a region of spontaneous limit-cycle oscillations (region B); see the *Appendix* for details. In region A, MPF is maintained primarily in its active form (as in metaphase arrest of mature oocytes), whereas in region C, it is maintained in inactive forms (as in the resting phase of nonproliferating somatic cells). In region B, MPF oscillates between active and inactive forms (Fig. 3*a*) with a period of 35 min, roughly the cell cycle length in early frog embryos. Throughout region B the oscillation period is given approximately by $([YT]_{max} - [YT]_{min})/(k_1[aa])$ and is only weakly dependent on k_4 and k_6. Thus, the oscillation period in the model is determined primarily by the rate of cyclin synthesis, as seems to be the case in early embryos. Furthermore, these oscillations are autonomous: they are not driven by temporal oscillations in parameter values, as might be caused by periodic DNA replication. Thus, these oscillations would persist even in the absence of periodic DNA synthesis (e.g., in enucleated frog eggs).

In the stippled region of Fig. 2, the division control system is excitable (Fig. 3*b*), and periodic fluctuations in k_4 or k_6 can excite periodic fluctuations in MPF and cyclin (Fig. 3*c*). Excitability of the steady state provides a mechanism for growth control of the division cycle. Unlike Fig. 3 *a* and *b*, where k_6 is held constant, in Fig. 3*c* I allow k_6 to be a function of time. Periodic changes in $k_6(t)$ induce periodic oscillations in MPF activity. In particular, I suppose that k_6 is proportional to the concentration of an enzyme that is being diluted out as the cell grows; i.e., $k_6(t)$ is proportional to $\exp(-0.693t/T_d)$, where T_d is the doubling time for cell growth. When $k_6(t)$ drops below a critical value (the boundary between regions B and C in Fig. 2), active MPF persists long enough for its autocatalytic action to induce massive dephosphorylation of the inactive stores of MPF accumulated during interphase. The abrupt increase in MPF activity presumably sets the division machinery in motion. As the store of MPF is activated, the flux through step 6 increases dramatically, and MPF is broken down. In this way, the control system generates a burst of MPF activation followed by MPF dissociation and cyclin degradation, paradoxically just at the time when the rate constant k_6 is at its lowest value. During S phase of the next cycle, replication of the gene for the enzyme catalyzing step 6 causes (I assume) a doubling in the amount of gene product,

Table 1. Kinetic equations governing the cyclin–cdc2 cycle in Fig. 1

$$d[C2]/dt = k_6[M] - k_8[\sim P][C2] + k_9[CP]$$
$$d[CP]/dt = -k_3[CP][Y] + k_8[\sim P][C2] - k_9[CP]$$
$$d[pM]/dt = k_3[CP][Y] - [pM]F([M]) + k_5[\sim P][M]$$
$$d[M]/dt = [pM]F([M]) - k_5[\sim P][M] - k_6[M]$$
$$d[Y]/dt = k_1[aa] - k_2[Y] - k_3[CP][Y]$$
$$d[YP]/dt = k_6[M] - k_7[YP]$$

t, time; k_i, rate constant for step i ($i = 1, \ldots, 9$); aa, amino acids. The concentrations [aa] and [$\sim P$] are assumed to be constant. There are six time-dependent variables: the concentrations of cdc2 ([C2]), cdc2-*P* ([CP]), preMPF = *P*-cyclin–cdc2-*P* ([pM]), active MPF = *P*-cyclin–cdc2 ([M]), cyclin ([Y]), and cyclin-*P* ([YP]). The activation of step 4 by active MPF is described by the function $F([M]) = k_4' + k_4([M]/[CT])^2$, where k_4' is the rate constant for step 4 when [active MPF] = 0 and k_4 is the rate constant when [active MPF] = [CT], where [CT] = total cdc2. I assume $k_4 >> k_4'$. This form of $F([M])$ is only one of many possible ways to describe the autocatalytic feedback of active MPF on its own production.

Table 2. Parameter values used in the numerical solution of the model equations

Parameter	Value	Notes
k_1[aa]/[CT]	0.015 min^{-1}	*
k_2	0	†
k_3[CT]	200 min^{-1}	*
k_4	10–1000 min^{-1} (adjustable)	
k_4'	0.018 min^{-1}	
k_5[$\sim P$]	0	‡
k_6	0.1–10 min^{-1} (adjustable)	
k_7	0.6 min^{-1}	†
k_8[$\sim P$]	$>>k_9$	§
k_9	$>>k_6$	§

*It is assumed that [CT] = [C2] + [CP] + [pM] + [M] = constant. For growing cells, this implies that cdc2 protein is continuously synthesized to maintain a constant concentration of cdc2 subunits (31).

†In the absence of evidence to the contrary, it is assumed that newly synthesized cyclin is stable ($k_2 = 0$). If $k_2 \neq 0$, the behavior of the model is basically unchanged, as long as $k_2 << k_3$[CT]. In accord with experimental evidence, I assume that cyclin-*P* subunits released from MPF complexes are quickly degraded (half-life $\simeq$ 1 min).

‡In all calculations reported here, I ignore rephosphorylation of the cdc2 subunit of active MPF (step 5). Similar results can be obtained with $k_5 \neq 0$.

§I assume that cdc2 protein is phosphorylated as soon as it dissociates from the active MPF complex—i.e., $k_8[\sim P] >> k_9 >> k_6$. This allows us to neglect the first differential equation in Table 1 (i.e., $d[C2]/dt = 0$) and $[C2] \simeq (k_9/k_8[\sim P])[CP] << [CP]$.

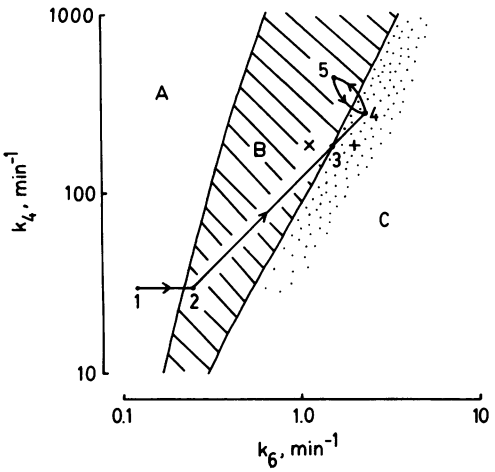

FIG. 2. Qualitative behavior of the cdc2–cyclin model of cell-cycle regulation. The control parameters are k_4, the rate constant describing the maximum rate of MPF activation, and k_6, the rate constant describing dissociation of the active MPF complex. Regions A and C correspond to stable steady-state behavior of the model; region B corresponds to spontaneous limit cycle oscillations. In the stippled area the regulatory system is excitable. The boundaries between regions A, B, and C were determined by integrating the differential equations in Table 1, for the parameter values in Table 2. Numerical integration was carried out by using Gear's algorithm for solving stiff ordinary differential equations (32). The "developmental path" **1 . . . 5** is described in the text.

so k_6 abruptly increases 2-fold. Continued cell growth causes $k_6(t)$ again to decrease, and the cycle repeats itself. The interplay between the control system, cell growth, and DNA replication generates periodic changes in $k_6(t)$ and periodic bursts of MPF activity with a cycle time identical to the mass-doubling time of the growing cell.

Figs. 2 and 3 demonstrate that, depending on the values of k_4 and k_6, the cell cycle regulatory system exhibits three different modes of control. For small values of k_6, the system displays a stable steady state of high MPF activity, which I associate with metaphase arrest of unfertilized eggs. For moderate values of k_6, the system executes autonomous oscillations reminiscent of rapid cell cycling in early embryos. For large values of k_6, the system is attracted to an excitable steady state of low MPF activity, which corresponds to interphase arrest of resting somatic cells or to growth-controlled bursts of MPF activity in proliferating somatic cells.

Midblastula Transition

A possible developmental scenario is illustrated by the path **1 . . . 5** in Fig. 2. Upon fertilization, the metaphase-arrested egg (at point **1**) is stimulated to rapid cell divisions (**2**) by an increase in the activity of the enzyme catalyzing step 6 (28). During the early embryonic cell cycles (**2** → **3**), the regulatory system is executing autonomous oscillations, and the control parameters, k_4 and k_6, increase as the nuclear genes coding for these enzymes are activated. At midblastula (**3**), autonomous oscillations cease, and the regulatory system enters the excitable domain. Cell division now becomes growth controlled. As cells grow, k_6 decreases (inhibitor diluted) and/or k_4 increases (activator accumulates), which drives the regulatory system back into domain B (**4** → **5**). The subsequent burst of MPF activity triggers mitosis, causes k_6 to increase (inhibitor synthesis) and/or k_4 to decrease (activator degradation), and brings the regulatory system back into the excitable domain (**5** → **4**).

Although there is a clear and abrupt lengthening of interdivision times at MBT, there is no visible increase in cell volume immediately thereafter (6, 20), so how can we entertain the idea that cell division becomes growth controlled after MBT? In the paradigm of growth control of cell division, cell "size" is never precisely specified, because no one knows what molecules, structures, or properties are used by cells to monitor their size. Thus, even though post-MBT cells

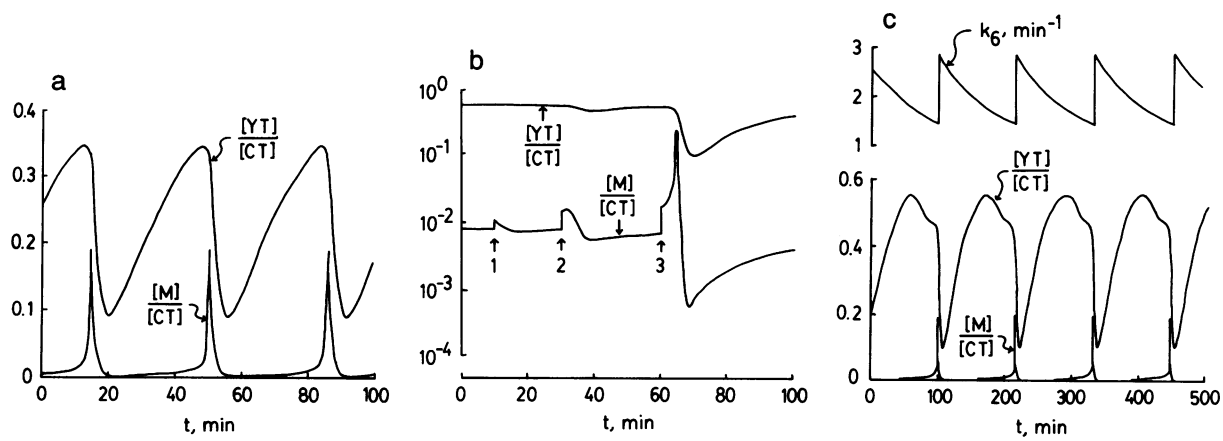

FIG. 3. Dynamical behavior of the cdc2–cyclin model. The curves are total cyclin ([YT] = [Y] + [YP] + [pM] + [M]) and active MPF [M] relative to total cdc2 ([CT] = [C2] + [CP] + [pM] + [M]). The differential equations in Table 1, for the parameter values in Table 2, were solved numerically by using a fourth-order Adams–Moulton integration routine (33) with time step = 0.001 min. (The adequacy of the numerical integration was checked by decreasing the time step and also by comparison to solutions generated by Gear's algorithm.) (*a*) Limit cycle oscillations for $k_4 = 180$ min^{-1}, $k_6 = 1$ min^{-1} (point × in Fig. 2). A "limit cycle" solution of a set of ordinary differential equations is a periodic solution that is asymptotically stable with respect to small perturbations in any of the dynamical variables. (*b*) Excitable steady state for $k_4 = 180$ min^{-1}, $k_6 = 2$ min^{-1} (point + in Fig. 2). Notice that the ordinate is a logarithmic scale. The steady state of low MPF activity ([M]/[CT] = 0.0074, [YT]/[CT] = 0.566) is stable with respect to small perturbations of MPF activity (at **1** and **2**) but a sufficiently large perturbation of [M] (at **3**) triggers a transient activation of MPF and subsequent destruction of cyclin. The regulatory system then recovers to the stable steady state. (*c*) Parameter values as in *b* except that k_6 is now a function of time (oscillating near point + in Fig. 2). See text for an explanation of the rules for $k_6(t)$. Notice that the period between cell divisions (bursts in MPF activity) is identical to the mass-doubling time (T_d = 116 min in this simulation). Simulations with different values of T_d (not shown) demonstrate that the period between MPF bursts is typically equal to the mass-doubling time—i.e., the cell division cycle is growth controlled under these circumstances. Growth control can also be achieved (simulations not shown), holding k_6 constant, by assuming that k_4 increases with time between divisions and decreases abruptly after an MPF burst.

may show no visible increase in volume, there may be within cells certain biochemical changes that are interpreted as growth. For instance, RNA synthesis turns on abruptly at MBT (5), and there is a dramatic rise in protein synthesis based on newly transcribed nuclear mRNA (34). A protein coded by this RNA rather than by maternal message could serve as a proxy for cell size, diluting out (or inactivating) the enzyme catalyzing step 6. Alternatively, in an activator-accumulation model, one of the post-MBT proteins could be the enzyme catalyzing step 4.

cdc25 and wee1

The parameters, k_4 and k_6, that govern the developmental path shown in Fig. 2 are rate constants determined by the concentrations of proteins that serve as an activator and an inhibitor, respectively, of MPF activity. The rate of activation of MPF is often associated with the level of expression of the *cdc25* gene (26, 35, 36), suggesting that k_4 be set proportional to the concentration of cdc25 protein. This association is encouraged by recent observations that cdc25 levels in fission yeast cells increase 3- to 4-fold during interphase and then drop abruptly at cell division (35). Exactly such behavior of k_4 can lead to growth-controlled cycles like those in Fig. 3*c* (simulations not shown).

Deactivation of MPF is often associated with the level of expression of *wee1* (10–12, 25). Recent evidence that wee1 can phosphorylate tyrosine residues (37) bolsters the suspicion that wee1 inhibits MPF by catalyzing step 5 and/or step 8 in Fig. 1. But, if this is the role of *wee1*, it is hard to understand how changing levels of expression of wild-type *wee1* can alter size at division, because, in the mathematical model, the magnitudes of k_5 and k_8 have very little effect on the dynamical behavior of the regulatory system. In contrast, size at division (in the model) is sensitively dependent on the magnitude of k_6. However, we cannot associate wee1 with step 6 because dysfunctional mutants at the locus controlling step 6 should block cells in mitosis, and this is clearly not the case for *wee1* mutations. It remains an open question to reformulate Fig. 1 so that *wee1* plays a more significant role in the control of division.

Discussion

To develop a precise mathematical model of cdc2–cyclin interactions, I have made many specific assumptions, some of which are crucial to the model and others inconsequential. Critical steps in the mechanism are the autocatalytic dephosphorylation of the cdc2 subunit (step 4) and breakdown of the active MPF complex (step 6). On the other hand, inhibition of MPF by rephosphorylating the cdc2 subunit (step 5) does not seem to be particularly significant or even necessary in this model. In all calculations reported here, $k_5 = 0$ but similar results are obtained for nonzero values of k_5. In particular, the "cycle control mode" (region A, B, or C in Fig. 2) is insensitive to the value of k_5 within broad limits.

Similarly, I have assumed that newly synthesized cyclin is stable ($k_2 = 0$), but the behavior of the model is not much changed when $k_2 \neq 0$, as long as proteolysis is considerably slower than dimerization ($k_2 << k_3$[CT]). It is crucial, however, to arrange that most cyclin be degraded in a brief interval just after MPF is activated (10, 12, 27, 28). In the model presented here, this arrangement is made by distinguishing between newly synthesized cyclin and cyclin subunits released when MPF dissociates. I imagine the distinction is made by phosphorylating cyclin when it is part of the MPF complex, but other modifications of cyclin would be possible. Another possibility is that cyclin subunits are never released from the MPF heterodimer but are proteolyzed while still bound to active (dephosphorylated) cdc2 (38). In this case I would interpret k_6 as the rate constant for *in situ* cyclin proteolysis. This simplifies the model without changing any of its fundamental characteristics.

In a different version of the model, no distinction is made between "new" and "used" cyclin subunits, but then it is necessary that active MPF stimulates the proteolysis of cyclin (27–29). MPF activation of cyclin degradation can be introduced into the model without making any changes in the qualitative behavior of the regulatory system (Fig. 2).

The autocatalytic nature of MPF activation {expressed by the function F([M]) in the model} is also essential for generating oscillations and excitability. From experiments with crude cytoplasmic extracts (17), it is not clear whether MPF stimulates its own activation directly or indirectly, but this uncertainty does not affect the kinetic model because F([M]) is only a formal description of the undisputed fact that MPF activation is autocatalytic. Of more importance mathematically is the *strength* of the autocatalytic effect, which is second order (quadratic) in the model. The nonlinearity of the effect seems to be important: all other things being equal, if F is a linear function of [M], oscillations and excitability are not evident (data not shown). However, other types of nonlinearity (for instance, replacing the linear kinetics of step 6 by Michaelis–Menten kinetics) in combination with first-order autocatalysis would probably be sufficient to generate oscillations and excitability like those observed in the model with second-order autocatalysis (39). The precise source and strength of the nonlinear control signals are important pieces of the puzzle that await careful experimentation *in vitro* with purified protein factors.

According to the model, the cell division cycle, under growth control, should show evidence of excitability. Advancement of mitosis in the acellular slime mold *Physarum polycephalum* in response to treatment with "F1 histone phosphokinase" (40) is a clear indication of the kind of excitability envisioned here. Another hallmark of excitable systems is their propensity to support traveling spatial waves of excitation (41). Traveling waves of mitotic activity are evident in fruit fly embryos (6), but it is not clear whether these are "trigger waves" (evidence of an underlying excitability) or "phase waves" (evidence of an underlying timing gradient) (41).

Though the overall scheme of Fig. 1 has firm genetic and biochemical support, many specific details of this version of the control system are speculative and may not stand the test of time. Nonetheless, as our understanding of the mechanism of cell-cycle control improves, mathematical analysis of precise models (42, 43) will play an increasingly important role in connecting molecular events with the integrated physiology of cell division.

Appendix: Phase Plane Analysis

Many features of Figs. 2 and 3 become clear when we rewrite the differential equations in Table 1. Let u = [M]/[CT], v = ([Y] + [pM] + [M])/[CT], w = ([pM] + [M])/[CT], and y = [YT]/[CT]. Then

$$du/dt = k_4(w - u)f(u) - k_6u, \quad [1]$$

$$dv/dt = (k_1[\text{aa}]/[\text{CT}]) - k_2(v - w) - k_6u, \quad [2]$$

$$dw/dt = k_3[\text{CT}](1 - w)(v - w) - k_6u, \quad [3]$$

$$dy/dt = (k_1[\text{aa}]/[\text{CT}]) - k_2(v - w) - k_7(y - v), \quad [4]$$

where $f(u) = \alpha + u^2$ and $\alpha = k_4'/k_4$. In deriving Eq. 3, we have used the facts that [CP] = $(1 - w)$[CT] − [C2] and [C2] << [CT] (see Table 2). Notice, first of all, that the first three equations can be solved independently of the fourth because

y does not appear in Eqs. 1–3. Second, because $k_3[CT] >> \max\{k_1[aa]/[CT], k_2, k_6\}$, w changes very rapidly compared to changes in v, so $w \simeq v$ as long as $0 < v < 1$. Thus, the cdc2–cyclin model reduces to a pair of nonlinear ordinary differential equations

$$du/dt = k_4(v - u)(\alpha + u^2) - k_6u \quad [5]$$

$$dv/dt = (k_1[aa]/[CT]) - k_6u. \quad [6]$$

Equations similar to Eqs. 5 and 6 were derived by Norel and Agur (43) on the basis of different assumptions about cdc2–cyclin interactions. In their study of the cell cycle of *P. polycephalum*, Tyson and Kauffman (44) formulated a hypothetical model of a "mitotic oscillator" that is identical to Eqs. 5 and 6: simply define $u = Y$ and $v = X + Y$ in their equation 3. From this point of view, our current understanding of cell-cycle regulation can be expressed as a modified version of the "Brusselator," a famous theoretical model of chemical oscillations (45).

Equations like Eqs. 5 and 6 are best analyzed by phase plane techniques (46). In the u-v plane (Fig. 4), I plot the locus of points where $du/dt = 0$,

$$v = u + k_6u/\{k_4(\alpha + u^2)\} \quad (\text{"}u\text{-nullcline"}) \quad [7]$$

and the locus of points where $dv/dt = 0$,

$$u = k_1[aa]/k_6[CT] \quad (\text{"}v\text{-nullcline"}). \quad [8]$$

The v-nullcline is just a vertical line. The u-nullcline is N-shaped with a local maximum near $u = \sqrt{k_4'/k_4}$, $v = k_6/2\sqrt{k_4'k_4}$ and a local minimum near $u = \sqrt{k_6/k_4}$, $v = 2\sqrt{k_6/k_4}$. (These estimates are reasonably accurate as long as $k_4'/k_6 < 0.025$.) To ensure that $v < 1$, we insist that $k_6 < 2\sqrt{k_4'k_4}$, which implies that k_4 must exceed 10 k_6. The requirements that $400\,k_4' < 10\,k_6 < k_4$ are satisfied by the parameter values in Table 2.

Steady states, where both $du/dt = 0$ and $dv/dt = 0$, lie at intersections of the nullclines. The nullclines may intersect in three qualitatively different ways (Fig. 4), which correspond to the three characteristic modes of the control system:

Mode A. Stable steady state with high MPF activity, when

$$k_1[aa]/k_6[CT] > \sqrt{k_6/k_4}.$$

Mode B. Unstable steady state (spontaneous oscillations), when

$$\sqrt{k_4'/k_4} < k_1[aa]/k_6[CT] < \sqrt{k_6/k_4}.$$

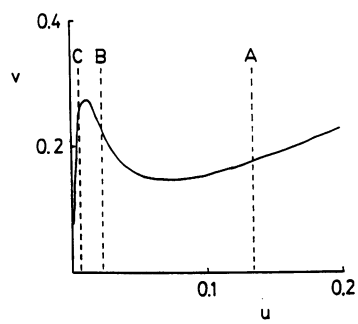

FIG. 4. The phase plane for Eqs. 5 and 6. Steady states occur at the intersections of the solid curve (the u-nullcline) and dashed lines (the v-nullcline for three different cases). A, stable steady state with high MPF activity; B, unstable steady state (limit cycle oscillations); C, excitable steady state with low MPF activity.

Mode C. Stable steady state with low MPF activity, when

$$k_1[aa]/k_6[CT] < \sqrt{k_4'/k_4}$$

The boundaries between regions A, B, and C in Fig. 2 are simply

$$\log k_4 = 3 \log k_6 - 2 \log(k_1[aa]/[CT])$$

$$\log k_4 = 2 \log k_6 - 2 \log(k_1[aa]/[CT]) + \log k_4'.$$

P. Nurse, K. Chen, M. Lederman, B. Novak, and an anonymous referee provided helpful critiques of the manuscript. This work was supported by the National Science Foundation (DMS-8810456) and the National Institutes of Health (GM-36809).

1. Mitchison, J. M. (1971) *The Biology of the Cell Cycle* (Cambridge Univ. Press, Cambridge, U.K.).
2. John, P. C. L., ed. (1981) *The Cell Cycle* (Cambridge Univ. Press, Cambridge, U.K.).
3. Nurse, P. & Streiblova, E., eds. (1984) *The Microbial Cell Cycle* (CRC, Boca Raton, FL).
4. Tyson, J. J. (1987) *J. Theor. Biol.* **126**, 381–391.
5. Newport, J. & Kirschner, M. W. (1982) *Cell* **30**, 675–686.
6. Foe, V. (1989) *Development* **107**, 1–22.
7. Hara, T., Tydeman, P. & Kirschner, M. W. (1980) *Proc. Natl. Acad. Sci. USA* **77**, 462–466.
8. Harvey, E. B. (1940) *Biol. Bull.* **79**, 166–187.
9. Mazia, D. (1974) *Sci. Am.* **230(1)**, 54–64.
10. Murray, A. W. & Kirschner, M. W. (1989) *Science* **246**, 614–621.
11. O'Farrell, P. H., Edgar, B. A., Lakich, D. & Lehner, C. F. (1989) *Science* **246**, 635–640.
12. Nurse, P. (1990) *Nature (London)* **344**, 503–508.
13. Moreno, S. & Nurse, P. (1990) *Cell* **61**, 549–551.
14. Lewin, B. (1990) *Cell* **61**, 743–752.
15. Draetta, G., Luca, F., Westendorf, J., Brizuela, L., Ruderman, J. & Beach, D. (1989) *Cell* **56**, 829–838.
16. Gautier, J., Minshull, J., Lohka, M., Glotzer, M., Hunt, T. & Maller, J. L. (1990) *Cell* **60**, 487–494.
17. Cyert, M. S. & Kirschner, M. W. (1988) *Cell* **53**, 185–195.
18. Gould, K. L. & Nurse, P. (1989) *Nature (London)* **342**, 39–45.
19. Evans, T., Rosenthal, E., Youngbloom, J., Distel, D. & Hunt, T. (1983) *Cell* **33**, 389–396.
20. Newport, J. W. & Kirschner, M. W. (1984) *Cell* **37**, 731–742.
21. Murray, A. W. & Kirschner, M. W. (1989) *Nature (London)* **339**, 275–280.
22. Minshull, J., Blow, J. & Hunt, T. (1989) *Cell* **56**, 947–956.
23. Ford, C. C. (1985) *J. Embryol. Exp. Morphol.* **89** (Suppl.), 271–284.
24. Gerhardt, J., Wu, M. & Kirschner, M. W. (1984) *J. Cell Biol.* **98**, 1247–1255.
25. Russell, P. & Nurse, P. (1987) *Cell* **49**, 559–567.
26. Russell, P. & Nurse, P. (1987) *Cell* **45**, 145–153.
27. Murray, A. W. (1989) *Nature (London)* **342**, 14–15.
28. Hunt, T. (1989) *Nature (London)* **342**, 483–484.
29. Felix, M.-A., Labbe, J.-C., Doree, M., Hunt, T. & Karsenti, E. (1990) *Nature (London)* **346**, 379–382.
30. Solomon, M. J., Glotzer, M., Lee, T. H., Philippe, M. & Kirschner, M. W. (1990) *Cell* **63**, 1013–1024.
31. Simanis, V. & Nurse, P. (1986) *Cell* **45**, 261–268.
32. Ermentrout, B. (1990) *PHASEPLANE, The Dynamical Systems Tool* (Brooks/Cole, Pacific Grove, CA), Version 3.0.
33. Kirchner, T. B. (1990) *TIME-ZERO, The Integrated Modeling Environment* (Quaternary Software, Fort Collins, CO).
34. Gross, P. R. & Cousineau, G. H. (1964) *Exp. Cell Res.* **33**, 368–395.
35. Moreno, S., Nurse, P. & Russell, P. (1990) *Nature (London)* **344**, 549–552.
36. Kumagai, A. & Dunphy, W. G. (1991) *Cell* **64**, 903–914.
37. Featherstone, C. & Russell, P. (1991) *Nature (London)* **349**, 808–811.
38. Murray, A. W., Solomon, M. J. & Kirschner, M. W. (1989) *Nature (London)* **339**, 280–286.
39. Higgins, J. (1967) *Ind. Eng. Chem.* **59**, 18–62.
40. Bradbury, E. M., Inglis, R. J., Matthews, H. R. & Langan, T. A. (1974) *Nature (London)* **249**, 553–556.
41. Tyson, J. J. & Keener, J. P. (1988) *Physica D* **32**, 327–361.
42. Hyver, C. & Le Guyader, H. (1990) *BioSystems* **24**, 85–90.
43. Norel, R. & Agur, Z. (1991) *Science* **251**, 1076–1078.
44. Tyson, J. & Kauffman, S. (1975) *J. Math. Biol.* **1**, 289–310.
45. Nicolis, G. & Prigogine, I. (1977) *Self-Organization in Nonequilibrium Systems* (Wiley, New York).
46. Edelstein-Keshet, L. (1988) *Mathematical Models in Biology* (Random House, New York), pp. 164–209.
47. Hunt, T. (1991) *Nature (London)* **349**, 100–101.
48. Glotzer, M., Murray, A. W. & Kirschner, M. W. (1991) *Nature (London)* **349**, 132–138.